RevMexAA (Serie de Conferencias), **32**, 115–119 (2008)

THE NATURE OF THE FAR-UV BREAK IN THE ENERGY DISTRIBUTION OF QUASARS

Luc Binette,[1] Sinhué Haro-Corzo,[2] Yair Krongold,[1] and Anja C. Andersen[3]

RESUMEN

Se observa un fuerte empinamiento en la distribución espectral de energía de los cuásares alrededor de 1100Å. Revisamos posibles interpretaciones para el origen físico de este quiebre en el ultravioleta lejano.

ABSTRACT

A prominent continuum steepening is observed in quasar energy distributions near 1100Å. We review possible interpretations for the physical origin of this so-called far-UV break.

Key Words: ISM: dust, extinction — galaxies: active — radiative transfer — ultraviolet: general

1. INTRODUCTION

The spectra of quasars and Seyfert galaxies show strong emission lines superimposed onto a bright continuum. The continuum contains a significant feature in the optical-ultraviolet region, known as "the Big Blue Bump" (BBB). Full coverage of the BBB region can only be gathered from significantly redshifted objects, since the Galaxy is opaque to the Lyman continuum. Although it has been possible to infer the UV Spectral Energy Distribution (SED) of quasars down to ~ 350 Å, it remains poorly known between the extreme UV and the X-rays. In the X-rays, a soft excess component is reported (Figure 1), which cannot be reduced to a simple extrapolation of the far-UV powerlaw (Haro-Corzo 2008 and Haro-Corzo et al. 2007, hereafter H07).

Composite energy distributions of the BBB were derived by Zheng et al. (1997) and later by Telfer et al. (2002, hereafter TZ02; reproduced in Figure 1) using archived HST-FOS spectra. Before averaging, each spectrum was dereddened for Galactic absorption as well as statistically corrected for the absorption due to intergalactic Lyα absorbers and Lyman limit systems. The transmission function for intergalactic absorption is illustrated in the inset of Figure 1 for redshifts 1, 2 and 3. Without such a correction, the far-UV continuum appears suppressed, as shown by the SDSS composite.

A striking feature of the composite quasar SED of TZ02 (see Figure 1) is that a significant steepening occurs around 1100Å, leading to a far-UV powerlaw of index $\nu^{-1.7}$ ($F_\nu \propto \nu^{+\alpha}$). Such a steepening of the continuum is present not only in composite SEDs,

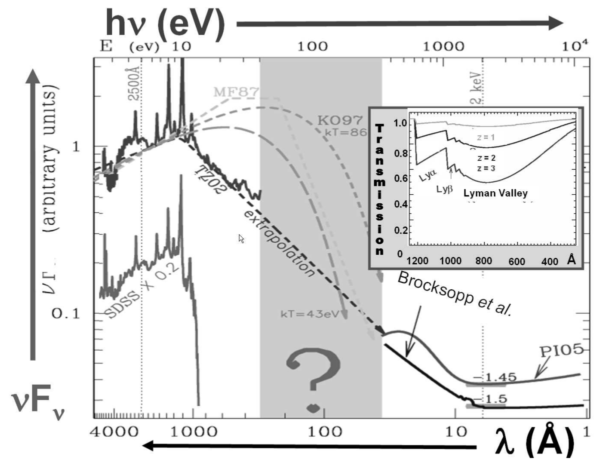

Fig. 1. Figure showing the UV composite spectra for quasars derived by TZ02 and SDSS (Vanden Berk et al. 2001) (the SDSS curve is moved down by 0.7 dex to avoid cluttering). The individual quasar spectra used in the TZ02 composite were divided by the transmission function (see inset) appropriate for their redshift before being averaged. The SDSS composite did not consider such a correction. Also shown are the averages of two series of X-ray models that fit individual XMM-Newton spectra. They correspond to the powerlaw+blackbody fits of Piconcelli et al. (2005, hereafter PI05) and to the broken power-law fits of Brocksopp et al. (2006), respectively. The vertical positions of these X-ray composites were arbitrarily set to reproduce an α_{OX} of -1.45 and -1.50, respectively. If, instead of composites, we considered SEDs from *individual* quasars, it could be shown that the extrapolation of the far-UV does *not* connect smoothly with the soft-X-ray excess component (see H07 for further details).

[1]Instituto de Astronomía, Universidad Nacional Autónoma de México, México D.F., México.

[2]Instituto de Ciencias Nucleares, Universidad Nacional Autónoma de México, México D.F., México.

[3]Dark Cosmology Center, Copenhagen, Denmark.

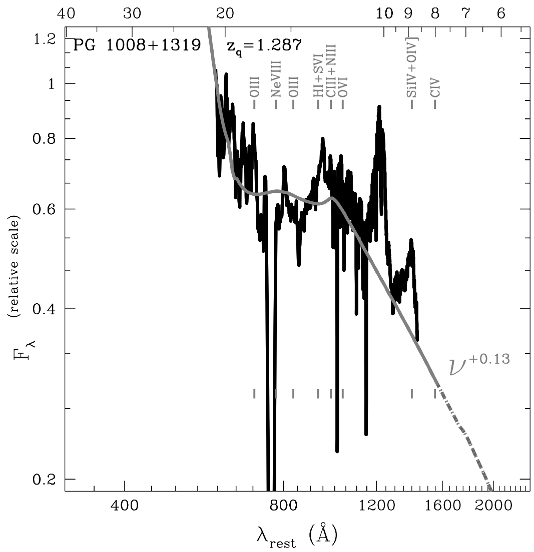

Fig. 2. Rest-frame spectrum of PG 1008+1319 (thin black line). The thick grey line represents an absorption model of a powerlaw SED, assuming extinction by cubic diamonds (using extinction curve D3 in H07).

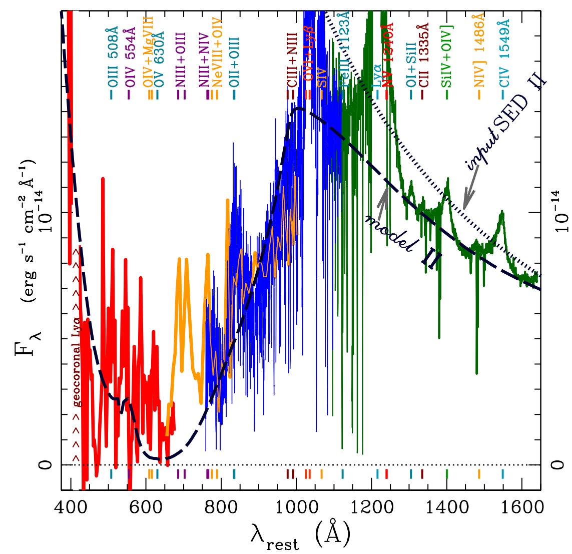

Fig. 3. Rest-frame spectrum of Ton 34 as derived from archive spectra from IUE, HST and Palomar (Sargent et al. 1988). The dash line represents an absorption model of the SED represented by the dotted line, assuming extinction by cubic nanodiamonds.

but is also evident in individual quasar spectra such as in PG 1148+549 (Figure 5) (see other examples in Binette et al. 2005; hereafter B05). The degree of steepening also varies significantly from object to object[4]. We will refer to this continuum steepening as the far-UV break. Korista, Ferland, & Baldwin (1997a, hereafter KO97) pointed out the difficulties of reproducing the equivalent widths of the high ionization lines of HeII λ1640Å, CIV λ1549Å and OVI λ1035Å, assuming a powerlaw as soft as ν^{-2}. State of the art photoionization models favor a much harder SED, one that peaks in the extreme-UV beyond 20 eV. In Figure 1, we show two theoretical SEDs characterized by an exponential cut-off of 43 and 86 eV. These were used in the BELR models of Korista et al. 1997b (see also Baldwin et al. 1995; Casebeer, Leighly, & Baron 2006). We will refer to this incongruity between the theoretical SEDs favored by photoionization and the steep far-UV SEDs actually observed as the 'softness problem'.

In our study of this problem, we have explored the shape of the far-UV break and whether it is followed by an upturn in the extreme UV, allowing the intrinsic SED to be much harder beyond 30 eV than suggested by an extrapolation of the far-UV continuum. If such an upturn existed, it would likely solve the softness problem identified above. In order to be able to evaluate the breath of the continuum break, that is, to identify a possible upturn in the extreme UV, we found that this was feasible using HST-FOS spectra, provided the quasars were of redshift $\simeq 1$ and had been observed with more than one grating. These conditions were met only for a few objects within the TZ02 sample that B05 analyzed. They reported an upturn in four quasars. One example, is PG 1008+1319 at $z = 1.287$ (Figure 2). After combining various archival spectra, Binette & Krongold (2008) reported a hint of a possible far-UV rise in a fifth object, Ton 34 ($z = 1.928$) (see Figure 3). This object is characterized by the largest steepening known ($F_\nu \propto \nu^{-5.3}$ in the far-UV). A sixth example is provided by the well studied quasar HE 2347−4342 ($z = 2.885$), where an upturn is visible shortward of 700Å as shown in Figure 6.

There is no generally accepted interpretation of the nature of the far-UV break. Below, in § 2, we review possible absorption mechanisms that would give rise to the break and furthermore allow the emergence of an upturn in the extreme-UV, in order to solve the 'softness problem' defined above.

2. POSSIBLE CAUSES FOR THE UV-BREAK

We hereafter assume that the far-UV break results from absorption and will consider two possibilities: [I]– HI (Lyα, β, γ ... + bound-free) and [II]– dust. We will consider four locations for

[4] Scott et al. (2004) reported a lack of evidence of a far-UV break in the case of nearby, less luminous AGN.

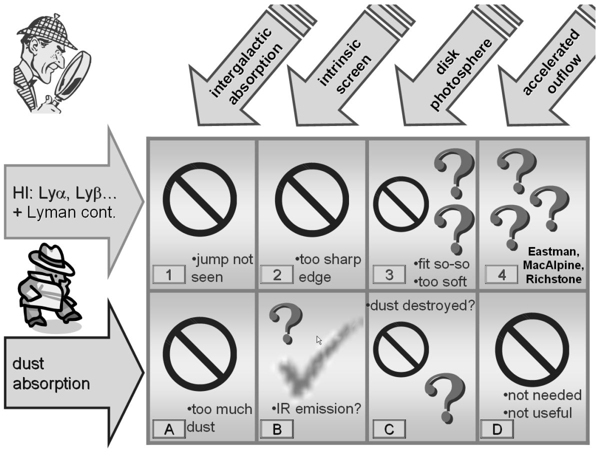

Fig. 4. Diagram illustrating the 8 possible *cases* arising from either HI or dust absorption. Barred circles denote rejected or unpromising cases, while question marks suggest a certain level of doubt or a conclusion that is possibly premature.

the absorbing medium: (*i*) intergalactic, (*ii*) local to the quasar ISM, (*iii*) accretion disk photosphere and (*iv*) accelerated outflow. The resulting eight cases are illustrated in Figure 4 with labels 1–4 for HI and A–D for the dust. Among the eight cases reviewed below, many impact positively the softness problem, either because the local BELR sees a different SED than the observer (e.g. intergalactic absorption), or because the absorption in the UV is followed by a flux upturn at higher energies.

Case 1 – Binette et al. (2003) studied the possibility of intergalactic HI absorption. They assumed a behavior of the HI density as a function of z proportional to the gas density expected from the warm-hot intergalactic medium. Although they could reproduce the steepening observed in the TZ02 composite, they rejected this possibility, since it implied a continuum flux discontinuity at 1216 Å (observer-frame) that is not observed.

Case 2 – An intrinsic absorber at a redshift close to the quasar results in a sharp absorption edge near 912 Å as well as in a saturated Lyα absorption line. A sharp edge at 912 Å has been reported in only ∼10% of AGN (see KO97) and is unrelated to the far-UV break discussed in this paper, which consists in a change in spectral index rather than a discontinuous edge. The situation described by case 2 is therefore not relevant to our study of the UV break.

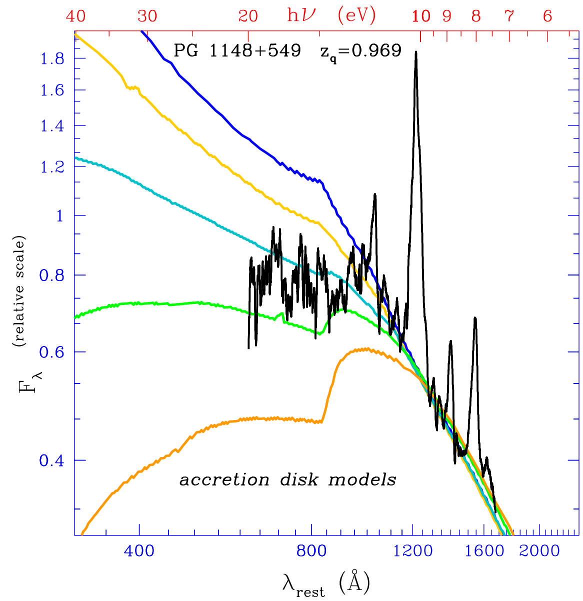

Fig. 5. The thin black line represents the far-UV spectrum of PG 1148+549. Five accretion disk models from Hubeny et al. (2000) are shown for comparison assuming a (face-on) stationary disk structure and a maximum rotating Kerr blackhole of mass $10^9\,M_\odot$, with accretion rates of 2, 1, 1/2, 1/4 and 1/8 $M_\odot\,\mathrm{yr}^{-1}$, respectively.

Case 3 – State of the art models of 'bare' accretion disks predict a steepening (i.e. a Lyman edge) near Lyα for a certain range of accretion rates and black hole masses. This is illustrated in Figure 5, where we show different SED models from Hubeny et al. (2000) that include a detailed non-LTE treatment of abundant elements as well as continuum opacities due to bound-free and free-free transitions. We find the fit to the far-UV break in PG 1148+549 to be unsatisfactory. A more important aspect to consider is that disk models that produce a break near the Lyman edge are not followed by a flux upturn at higher energies. Hence the softness problem remains whole with current disk models that intend to reproduce the break. A similar shortage of hard photons also characterizes the comptonized accretion disk model proposed by Zheng et al. (1997), even though in that case the UV break is much better reproduced. We may conjecture that current stationary disks fail, because they do not include thermal inhomogeneities, Parker instabilities or other energy transport mechanisms (Blaes 2007). Therefore, we cannot rule out that the next generation of disk models will succeed to simultaneously be very efficient in the far-UV and yet produce a trough near the Lyman limit. Both

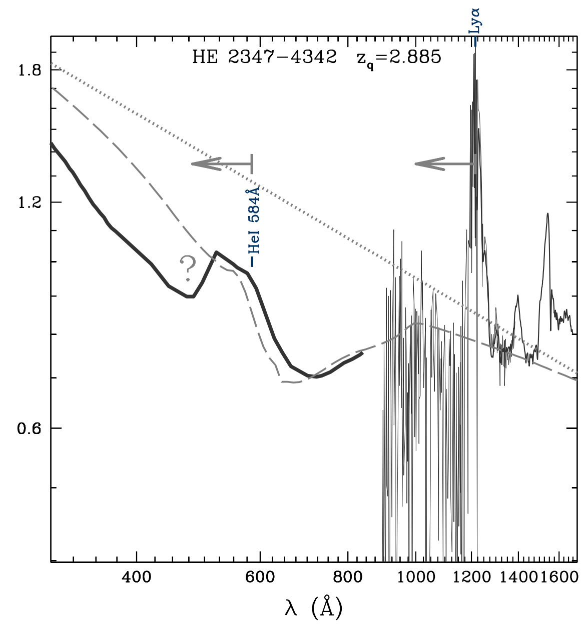

Fig. 6. Spectrum of HE 2347−4342 (thick and thin black lines) extracted from Reimers et al. (1998). The dashed line represents an absorption model of the SED represented by the dotted line, assuming extinction by cubic nanodiamonds.

of these features are required to fit the SED of HE 2347−4342 (Figure 6). Disks are also expected to generate a wind (see Proga 2007a, and references therein). Because a reduction of the surface temperature might be expected at the point where the wind is launched as a result of reduced viscous heating, we may speculate that a narrow disk wind (Proga 2007b), if launched from the position where the bulk of the 1000 Å flux originates, might cause an absorption trough where the break is observed.

Case 4 – Eastman, MacAlpine & Richstone (1983) produced a steepening of the continuum at 1200 Å by integrating the absorption from clouds progressively accelerated up to 0.8c. Such a model, after inclusion of cloud emission, is represented by the thick grayed line in Figure 7. A more thorough exploration of this type of model would be needed to determine whether it is a promising avenue. Would a wind structure rather than discrete clouds not be preferable? A different behavior of the HI opacity with velocity might be able to shift the break position to the observed value near 1100 Å (instead of $\simeq$ 1216Å). The upturn in flux beyond 20 eV also remains to be calculated. If HeI opacity were included, such models might succeed in explaining the odd dip observed at 500 Å in HE 2347−4342,

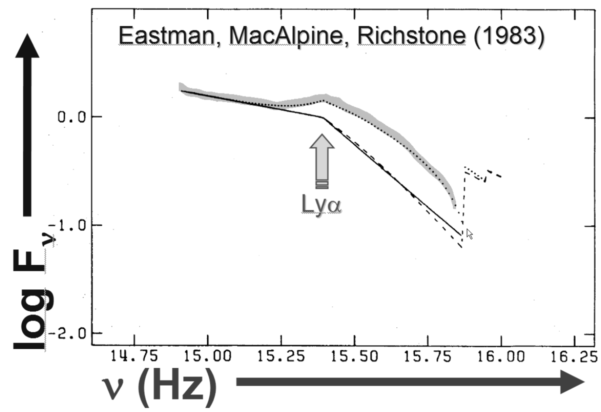

Fig. 7. The accelerated cloud absorption model (top grayed line) proposed by Eastman, MacAlpine, & Richstone (1983).

one of the most studied quasars (see Figure 6). Interestingly, both breaks at 1100Å and 500Å are blueshifted with respect to rest-frame Lyα from HeI and HI, at 584 Å and 1216 Å, respectively.

Case A – B05 studied the possibility of absorption by intergalactic dust consisting of nanodiamond grains (other dust compositions were unsuccessful). They could reproduce the wide dip centered on $z \simeq 1$ displayed by the far-UV indices α_{FUV} when plotted with redshift (Figure 12 in B05). This possibility was rejected, since it required too much intergalactic dust ($\sim$ 17% of all cosmic carbon!).

Case B – Shang et al. (2005) previously explored the possibility of ISM and SMC-like extinction to explain the break. They rejected this hypothesis, because the absorption resulted in a broad curvature for the SED, which is not observed. Assuming a dust component composed of crystallite carbon grains, B05 successfully reproduced the far-UV break observed in individual quasars of the TZ02 sample. The case of PG 1008+1319 is illustrated in Figure 2. The softness problem disappears, since the dust becomes transparent at higher energies and a flux upturn is therefore predicted below 650 Å. This allows the intrinsic SED to be much harder in the extreme UV than the flux measured next to the break suggests. Two other examples of an upturn in the extreme UV are presented here: Ton 34 (Figure 3) and HE 2347−4342 (Figure 6).

Case C – B05 found that the column of dust required to fit the far-UV break was about the same for the majority of their quasars. This is an improbable situation for the above case B, where the dust screen is presumed independent of the continuum source. Such a narrow range in dust opacities would make more sense if the dust screen was somehow connected to the continuum source. What about the possibility of the dust being part of the plasma where the UV is produced? Even though nanodiamond formation is favored by the presence of UV radiation[5] (Duley & Grishko 2001; Kouchi et al. 2005), the high temperatures of the inner disk coupled with its high gas density would certainly destroy the dust before it reaches the radius where the UV is radiated. We can therefore rule out this possibility. An interesting variant of case C that cannot so easily be ruled out is provided by having the dust manufactured within the much cooler outer regions of the disk and then launched as part of a funneled disk wind. We may conjecture that this dusty wind would later intercept our line-of-sight to the inner UV-emitting regions of the disk.

Case D – We consider the hypothesis of acceleration of dusty material to *high* velocities superfluous, for it is neither needed nor useful for the purpose of reproducing the far-UV break.

3. DISCUSSION

Crystallite carbon dust has not been yet observed in emission in the mid-IR. De Diego et al. (2007) actually ruled out meteoritic nanodiamond emission in 3C298 using *Spitzer* data. H07 has modified the original model of B05 by discarding meteoritic nanodiamonds and making use of cubic nanodiamonds only (i.e. gains without surface adsorbates). Attempts will be made to detect emission due to bulk impurities from this type of grains. A possible problem of the dust screen model is the absence of absorption lines associated with the dust screen (but see Binette & Krongold 2008).

To summarize, out of the 8 possibilities of Figure 4, we favor case B as our overall favored model. This is possibly more a reflection of this case having been a simpler paradigm to develop and later closely compared with the spectra. We consider the remaining three alternative cases 3, 4 and C as certainly worth being explored further.

This work was funded by the CONACyT grants J-49594 and J-50296, and the UNAM PAPIIT grant IN118905. The Dark Cosmology Centre is funded by the Danish National Research Foundation.

[5]It is interesting to note that via the mid-IR emission bands observed at 3.43 and 3.53μm (van Kerckhoven et al. 2002), nanodiamonds have so far only been identified around 3 stellar disks that turn out to be heated by the UV radiation from the central star.

REFERENCES

Baldwin, J., Ferland, G., Korista, K., & Verner, D. 1995, ApJ, 455, L119
Binette, L., Rodríguez-Martínez, M., Haro-Corzo, S., & Ballinas, I. 2003, ApJ, 590, 58
Binette, L., Magris C. G., Krongold, Y., Morisset, C., Haro-Corzo, S., de Diego, J. A., Mutschke, H., & Andersen, A. 2005, ApJ, 631, 661 (B05)
Binette, L., & Krongold, Y. 2008, A&A, 478, 739
Blaes, O. 2007, in ASP Conf. Ser. 373, The central engine of Active Galactic Nuclei, ed. L. C. Ho & J.-M. Wang (San Francisco: ASP), 75
Brocksopp, C., et al. 2006, MNRAS, 366, 953
Casebeer, D. A., Leighly, K. M., & Baron, E. 2006, ApJ, 637, 157
de Diego, J. A., Binette, L., Ogle, P., Andersen, A. C., Haro Corzo, S., & Wold, M. 2007, A&A, 467, L7
Duley, W. W., & Grishko, V. I. 2001, ApJ, 554, L209
Eastman, R. G., MacAlpine, G. M., & Richstone, D. O. 1983, ApJ, 275, 53
Haro-Corzo, S., Binette, L., Krongold, Y., Benitez, E., Humphrey, A., Nicastro, F., & Rodriguez-Martinez, M. 2007, ApJ, 662, 145 (H07)
Hubeny, I., Agol, E., Blaes, O., & Krolik, J. H. 2000, ApJ, 533, 710
Korista, K., Ferland, G., & Baldwin, J. 1997a, ApJ, 487, 555 (KO97)
Korista, K., Baldwin, J., Ferland, G., & Verner, D. 1997b, ApJS, 108, 401
Kouchi, A., Nakano, H., Kimura, Y., & Kaito, C. 2005, ApJ, 626, L129
Piconcelli, E., et al. 2005, A&A, 432, 15 (PI05)
Proga, D. 2007a, in ASP Conf. Ser. 373, The central engine of Active Galactic Nuclei, ed. L. C. Ho & J.-M. Wang (San Francisco: ASP), 267
———. 2007b, ApJ, 661, 693
Sargent, W. L. W., Boksenberg, A., & Steidel, C. C. 1988, ApJS, 68, 539
Shang, Z., et al. 2005, ApJ, 619, 41
Reimers, D., Köhler, S., Hagen, H.-J., & Wisotzki, L. 1998, Ultraviolet Astrophysics Beyond the IUE Final Archive, ESA SP-413, ed. W. Wamsteker & R. Gonzalez Riestra (Noordwijk: ESA), 579
Scott, J. E., Kriss, G. A., Brotherton, M., Green, R. F., Hutchings, J., Shull, J. M., & Zheng, W. 2004, ApJ, 615, 135
Telfer, R. C., Zheng, W., Kriss, G. A., Davidsen, A. F. 2002, ApJ, 565, 773 (TZ02)
Vanden Berk, D. E., et al. 2001, AJ, 122, 549
van Kerckhoven, C., Tielens, A. G. G. M., Waelkens, C. 2002, A&A, 384, 568
Zheng, W., Kriss, G. A., Telfer, R. C., Grimes, J. P., & Davidsen, A. F. 1997, ApJ, 475, 469